

# Performance Comparison of Stand Alone Solar PV System with Variable Step Size MPPT

Shiny Paul\*, Poulouse Jacob\*\*, Josephkutty Jacob\*\*

\* Division of Electrical Engineering, Cochin University of Science and Technology, Kerala, India

\*\*Department of Computer Science, Cochin University of Science and Technology Kochi, Kerala, India

\*\* Division of Electrical Engineering, Cochin University of Science and Technology, Kerala, India

(shiny paulj@cusat.ac.in, [kpj@cusat.ac.in](mailto:kpj@cusat.ac.in), josephkutti@cusat.ac.in)

Poulouse Jacob, Professor & Dean, Department of Information Technology, Rajagiri School of Engineering & Technology, Rajagiri Valley, Kakkanad., Kochi 682 039 Kerala

Fax: +91 484 2426241, [kpj@cusat.ac.in](mailto:kpj@cusat.ac.in)

*Received: 31.07.2020 Accepted: 01.09.2020*

**Abstract-** The nonlinear behavior of Photo Voltaic (PV) module with respect to the output parameters like current, voltage and power depends mainly on climatic conditions like solar irradiation and air temperature of the location. PV sources can develop only low DC voltage and so consumers cannot rely directly on them for their power requirement. To improve the voltage magnitude of the PV source within a certain limit, cells may be connected in series. To improve the voltage further, it is feasible to include a DC to DC converter in the system with good power efficiency. This DC to DC converter connected to the PV module does the job of a power conditioning unit which transfers power to the load. To transfer maximum power, the conditioning unit maintains its input impedance constant with the support of a Maximum Power Point Tracking (MPPT) controller irrespective of the change in load. An MPPT controller locates the point of maximum power of the PV module and hence controls the operating point of the converter. The quality of the power obtained at the output has specific dependence on the type of converter and controller used in the PV system. There are various ongoing researches using different controller techniques searching scope of efficient utilization of energy from a PV source [1, 2]. Among them, Variable Step Size (VSS) P&O MPPT controller performs superior in a PV system because of its efficiency in locating the exact point of maximum power output of the PV module with minimum oscillations around the operating point, good tracking speed and with the added advantage of ease in implementation [3, 4]. In this paper, a standalone PV system is modelled with three different converter topologies and its performance is analyzed using variable step size MPPT. Performance comparison is done in terms of input current ripple, output voltage ripple, output power ripple and efficiency. A detailed simulation is done for different climatic conditions in MATLAB/Simulink and the results obtained are presented.

**Keywords:** Standalone PV, Converter topologies, SSHG, SEPIC, Modified SEPIC, VSS P&O MPPT

## 1. Introduction

At present the target of meeting energy needs of the day without badly affecting the ability of the future world to manage its energy requirement is a vital concern. To attain a sustainable situation with respect to energy, due attention should be considered for the management of efficient methods for the extraction of energy without being a challenge for safety of the atmosphere. As per the available records a large

percentage of greenhouse gas emission [5] is the result of the means used for the production of energy. Among all sustainable energy resources, solar energy, the inexhaustible energy, is a powerful source. Moreover, electrification of remote places to which transmission of power turns out to be a tedious task can be compromised by the efficient and cost effective methods of extraction of solar energy from the location. Solar energy is a source which is unique among the rest energy sources for having no greenhouse gas emission

along with added features like clean source, plenty in availability and nonpolluting nature. The system used for the conversion of solar energy to electric energy has the following components viz, PV module, controller and converter. Block diagram of the PV system is shown in Fig.1 [6].

The PV module which converts solar energy to electric energy has the main drawback of low energy efficiency. An MPPT controller is required to extract maximum power and hence to increase the energy efficiency of the solar PV for any input condition.

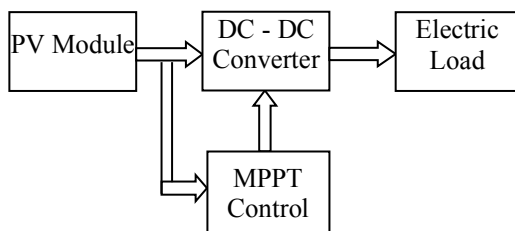


Fig. 1. Block diagram of solar PV system

The voltage gain ratio of the converter can be increased by increasing the value of duty cycle ratio but, with a sacrifice on the power efficiency of the system. To improve the voltage gain without affecting the power efficiency and hence to transfer maximum power to the load, various converter topologies and controller techniques are proposed [7, 8, 9]. In this paper performance of the proposed PV system is analyzed using three non-isolated DC-DC converter topologies like Single Switch High Gain (SSHG), Single Ended Primary Inductor (SEPIC) and Modified SEPIC converter. A variable step size MPPT controller is chosen for the proposed system.

SSHG converter is a modified form of conventional Boost converter with less input current ripple. The added diode and the capacitor components reduces voltage stress on the switch. For a 250W, 30/300V SSHG converter, full load efficiency is 92.20%. [10]. This converter topology provides high voltage gain without using a transformer. Hence cost and size of the converter is minimized [11]. SEPIC topologies can increase the output voltage to five times that of the input when the duty cycle ratio is set as 0.82. To increase the output voltage to ten times that of the input for the same duty cycle ratio, a modified SEPIC topology with an efficiency of 91.5% is proposed [12]. All these converter topologies can effectively be applied to a PV system.

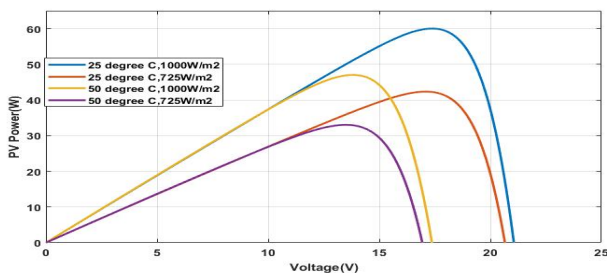


Fig. 2. Output characteristic of the PV module

Typical P-V characteristic of the proposed MSX60 PV module for different air temperature and solar irradiation is

shown in Fig. 2. Section 2 describes PV modelling, section 3 describes the algorithm used for the selected MPPT controller, different converter topologies used for system performance comparison are described in section 4. Performance analysis of the system is done in section 5 based on the outcome from the numerical experiments and section 7 concludes the work.

## 2. Modeling of PV system

Silicon based cells which are the basic elements of a PV module can be designed for any voltage/current requirement. This requirement can be achieved by the interconnection of the required number of cells in parallel or series. They are capable of converting solar energy to electric energy when exposed to daylight, whose irradiation and/or air temperature causes change in the magnitude of electric energy obtained at the output [13, 14, 15]. Equivalent circuit of the PV cell for the considered system is shown in Fig. 3 [16]. It consists of photo current ( $i_{pv}$ ), diode current ( $i_d$ ), terminal current ( $i$ ) and terminal voltage ( $V$ ).

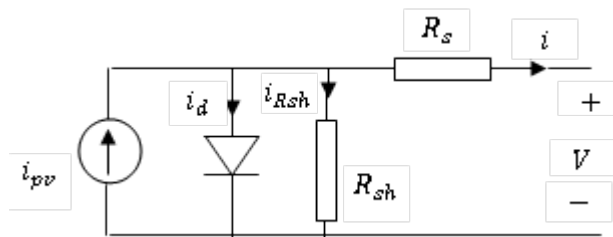


Fig. 3. Model of the PV cell

For modelling the PV source, P-V characteristic plays a significant roll [17]. In addition to the already mentioned factors like solar irradiation ( $G$ ) and air temperature, other factors like PV cell combination, series resistance ( $R_s$ ), shunt resistance ( $R_{sh}$ ) ideality factor of diode ( $A$ ), short circuit current ( $I_{sc}$ ) of the module at Standard Test Conditions ( $STC$ ), temperature coefficient of short circuit current ( $K_i$ ) also should be considered [18, 19]. Light generated current of the PV cell which depends on solar irradiation and cell temperature in Kelvin ( $T_c$ ) is expressed in Eq. (1), where  $T$  is the reference temperature (298.15 Kelvin). Terminal current and terminal voltage of the cell is represented by Eq. (2) and Eq. (3) respectively [15].

$$i_{pv} = I_{sc} + K_i(T_c - T)G \quad (1)$$

$$i = i_{pv} - I_s \left[ \exp \left[ \frac{qV + qR_s i}{AKT_c} \right] - 1 \right] - \left[ \frac{V + R_s i}{R_{sh}} \right] \quad (2)$$

$$V = i_{pv}R_{sh} - iR_{sh} + I_s \left[ \exp \left[ \frac{qV + qR_s i}{AKT_c} \right] - 1 \right] - iR_s \quad (3)$$

For the proposed model it is observed that as the solar irradiation increases, output current and voltage increases, resulting in an increase in output power of the module. Meanwhile, if air temperature increases a prominent decrease in output voltage with only a marginal rise in current. This results in an overall decrease in output power [20].

**3. Variable step size MPPT controller**

The dependency of PV cells on the solar irradiation and air temperature promises only a low power efficiency (<20%). This drawback along with its typical nonlinear P-V characteristics with only one operating point corresponding to maximum power indicates the importance of locating this Maximum Power Point (MPP). So to improve the power efficiency of PV source, it is required to continuously track this MPP for any climatic condition [21, 22].

MPPT algorithm is described in different literatures with different viewpoint like tracking speed, sensing parameters, type of sensors, economy etc. Classification of MPPT techniques based on offline and online methods are done in paper [23]. With large number of MPPT techniques available, it is necessary to have a comparison of them so that best MPPT is selected for a particular application [24]. In this paper it is stated that P&O algorithm which uses simple control strategy is easy to implement, locates MPP by sensing instantaneous values of voltage and current. Tracking speed of this algorithm is decided by the duration of perturbation.

In conventional Perturb and Observe (P&O) MPPT [25, 26, 27, 28] a constant value of perturbation is used for varying the duty cycle throughout the process of fetching the maximum power by locating MPP. Though simplest among all MPPT techniques, it possesses defects like inefficiency in locating exact MPP, oscillations around MPP caused by the fluctuation of power around MPP etc. To overcome these limitations, perturbation in the sensed voltage can be reduced. But this will increase the time taken by the controller to fetch the MPP. Hence the proposed VSS P&O MPPT controller is incorporated in the system. Here, two different perturbation values for duty cycle is considered in the process of locating MPP. When the operating point is away from MPP, large perturbation value is considered and if near to it, small perturbation value is considered [24, 29, 30].

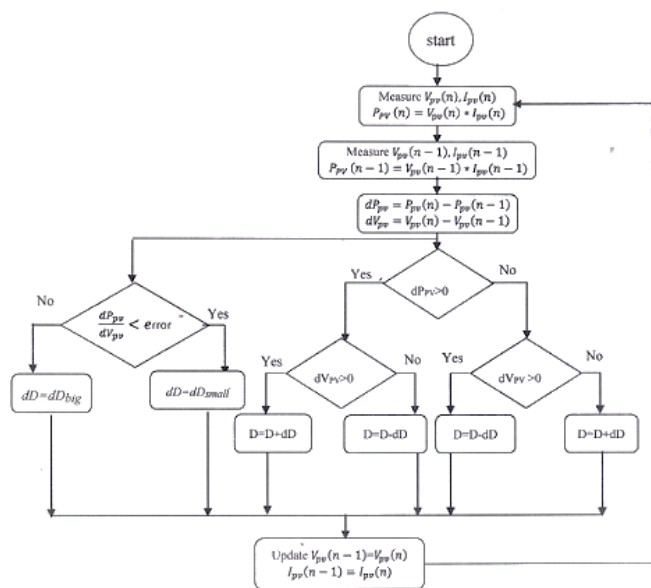


**Fig. 4a** Flow chart of Variable step size P&O algorithm

Figure 4a shows [31] the flowchart of the proposed controller and Fig. 4b shows the Simulink model of this controller used in the system. Here a continuous monitoring of change in voltage ( $dV_{pv}$ ) and change in power ( $dP_{pv}$ ) is done and ( $dP_{pv}/dV_{pv}$ ) is calculated and it is compared with an error value. For a large value of the ratio, the step value is made large (0.02) and if the operating point is near MPP, a small value of perturbation (0.005) is used. The purpose of the proposed MPPT is to control the duty cycle of the converter. This is done in such a manner that the actual load seen by the PV source (input impedance of converter) is made same as that of load at which maximum power is extracted from the PV source.

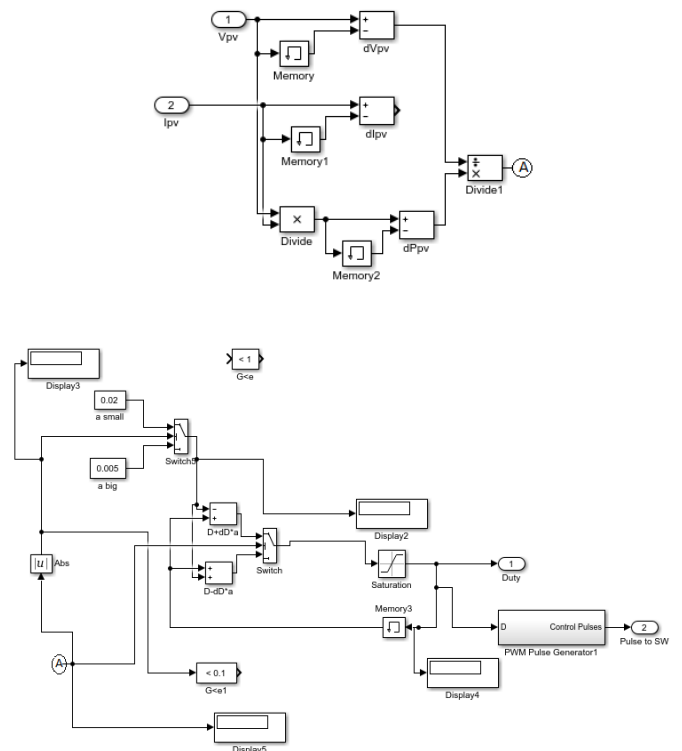


**Fig. 4b** Electrical model of VSS P&O MPPT

**4. Converter topologies used in the System**

The three converter topologies used in the system for the comparative analysis is designed with the specification, 16/24V, 60 W, 9.6 Ω load for a switching frequency  $f_s$  of 10kHz using circuit components like inductors  $L_1, L_2$  with voltage across them represented as and respectively, capacitors  $C, C_1, C_2, C_3$  and  $C_0$  with the corresponding voltage across them represented as,  $V_i, V_{C1}, V_{C2}, V_{C3}$  and  $V_0$  respectively. A brief description of the converters used is given below.

**4.1 Single Switch High gain (SSHG) converter**

Schematic diagram of the converter shown in Fig. 5 [10, 32] has four modes of operation in one cycle of switching. Among them three modes for ON state ( $T_{ON}$ ) and the rest mode for the off duration ( $T_{OFF}$ ) of the switch.

Mode 1

During this operating mode, D<sub>3</sub> forward biased and D<sub>1</sub>, D<sub>0</sub>, D<sub>2</sub> remains reverse biased. Capacitors C<sub>1</sub> and C<sub>2</sub> get charged. The output voltage is maintained as V<sub>0</sub> because of the discharging action of C<sub>0</sub>. This operation ends when current through D<sub>3</sub> becomes zero.

Mode 2

For this mode of operation all the diodes are reverse biased. Inductor L<sub>1</sub> still gets charged from input voltage V<sub>i</sub>. V<sub>0</sub> is maintained by the discharge of C<sub>0</sub>. This mode ends when the polarity of L<sub>2</sub> gets reversed and when diode D<sub>2</sub> becomes forward biased.

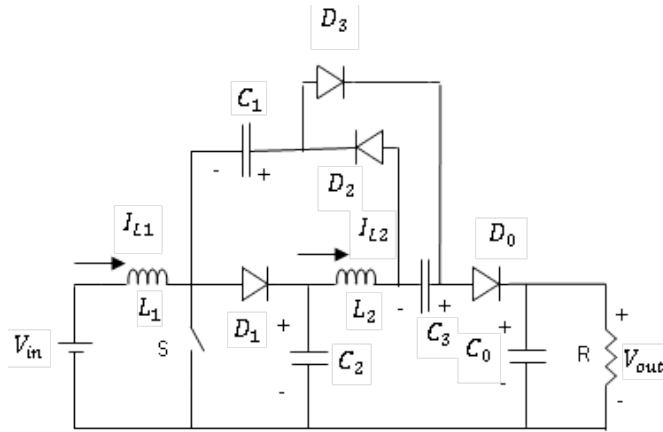


Figure 5. Single Switch High Gain Converter

Mode 3

The switch is still in the ON state, D<sub>2</sub> forward biased, but D<sub>1</sub>, D<sub>3</sub>, D<sub>0</sub> remains as it was in the previous mode. Output voltage V<sub>0</sub> remains constant by the action of C<sub>0</sub>. As the polarity of L<sub>2</sub> get reversed, now D<sub>1</sub> becomes forward biased and then C<sub>1</sub> gets charged. This mode ends up when the switch is in OFF state, so current through D<sub>2</sub> becomes zero.

Mode 4

Now when the switch is in OFF state, D<sub>2</sub> is reverse biased and D<sub>1</sub>, D<sub>3</sub>, D<sub>0</sub> forward biased. Now L<sub>1</sub>, L<sub>2</sub> starts discharging energy from them and C<sub>1</sub> gets charged. C<sub>0</sub> starts charging from C<sub>3</sub> through D<sub>0</sub>. This mode ends when C<sub>0</sub> gets completely charged and when the MOSFET switch is turned ON. The following equations apply for the two states of switch.

When S is ON (Mode 1, 2, 3)

$$V_{L1} = V_i \tag{4}$$

$$V_{L2} = V_{C2} - V_{C1} \tag{5}$$

When S is OFF (Mode 4)

$$V_0 = V_{C2} + V_{C1} \tag{6}$$

$$V_{L1} = V_i - V_{C2} \tag{7}$$

$$V_{C1} - V_{C3} + V_{L2} = 0 \tag{8}$$

During steady state, average voltage across inductor L<sub>1</sub> in one switching cycle is zero, which is expressed as

$$V_i DT_s + (V_i - V_{C2})(1 - D)T_s = 0 \tag{9}$$

D is the duty cycle and T<sub>s</sub> is the switching period.

$$\frac{V_{C2}}{V_i} = \frac{1}{1-D} \tag{10}$$

Eq. (10) is the gain equation of the Boost Converter.

When similar condition is applied to inductor L<sub>2</sub> the following equations are derived

$$(V_{C2} - V_{C1})DT_s + (V_{C2} + V_{C3} - V_0)(1 - D)T_s = 0 \tag{11}$$

$$\frac{V_0}{V_i} = \frac{3+D}{2(1-D)} \tag{12}$$

Eq. (12) is the gain equation of the proposed Converter.

It is inferred that the gain of the proposed converter is many times higher than that of a Boost converter and this is achieved by varying the duty cycle.

Design Considerations

Comparing Eq. (6) and (7), duty cycle

$$D = \frac{1 - V_i}{V_{C2}} \tag{13}$$

$$V_{C2} = \frac{V_0 + V_i}{2} \tag{14}$$

For the converter with chosen rating, D = 0.2

$$L_1 = \frac{V_i DT_s}{\Delta I_{LON}} = 284 \mu H \tag{16}$$

$\Delta I_{LON}$  is the ripple current through L<sub>1</sub> when the switch is in the ON state and is equal to 30% of current through L<sub>1</sub>, when switch is ON,  $I_{LON} = I_i = 3.75 A$ .

$$L_2 = \frac{V_{C2}(1-D)T_s}{\Delta I_{LOFF}} = 1422 \mu H \tag{17}$$

Design of capacitor

$$C_1 = C_2 = C_3 = \frac{I_0 D}{f_s \Delta V_{C2}} = 25 \mu F$$

Where I<sub>0</sub> is the output current.

$$\Delta V_{C2} = 10\% \text{ of } V_{C2} = 2V$$

$$C_0 = \frac{I_0 D}{f_s \Delta V_0} = 41.6 \mu F$$

4.2 Single Ended Primary Inductor Converter (SEPIC)

Since the solar PV system with SSHG converter offers low efficiency, it is replaced by SEPIC converter. The operation of this converter is based on the principle of step-up and step down converters. Schematic diagram of the converter shown in Fig. 6 [33, 34] has two modes of operation in one cycle of switching. The converter has two inductors L<sub>1</sub> and L<sub>2</sub> for buck or boost operation of the input and offers a non-inverted output with a high static gain.

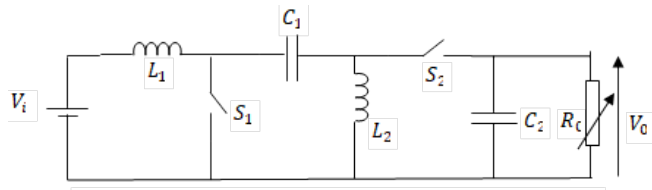


Figure 6. Single ended primary inductor converter

The two modes of operation of the converter are given below.

Mode 1 ( $S_1$  ON and  $S_2$  OFF)

$$V_i = V_{L1} \tag{18}$$

$$V_{L2} = -V_{C1} \tag{19}$$

Mode 2 ( $S_1$  OFF and  $S_2$  ON)

$$V_{L1} = V_i - (V_{C1} + V_{C2}) \tag{20}$$

$$V_{L2} - V_{C2} = 0 \tag{21}$$

Average voltage across the inductor during one switching cycle is equal to zero and hence the following equations.

$$V_i DT_s + [V_i - (V_{C1} + V_{C2})](1 - D)T_s = 0 \tag{22}$$

$$-V_{C1}T_{ON} + V_{C2}T_{OFF} = 0 \tag{23}$$

$$V_{C1} = \frac{V_{C2}}{D}(1 - D) \tag{24}$$

$$\frac{V_0}{V_i} = \frac{V_{C2}}{V_i} = \frac{D}{1 - D} \tag{25}$$

This gives the gain equation of the SEPIC converter.

Design considerations

Considering Eq. (25), duty cycle,  $D = 0.6$ .

From Eq. (16),  $L_1 = 853\mu H$

From Eq. (25),  $V_{C2} = 24V$

$L_2 = 853\mu H$ ,  $C = 17.5\mu F$ ,  $C_1 = C_0 = 121\mu F$

#### 4.2 Modified SEPIC Converter

The schematic diagram of the converter is shown in Fig. 7 [12, 35] and it has two modes of operation.

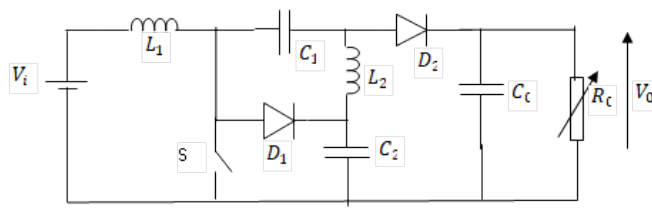


Figure 7 Modified SEPIC converter

Mode 1. When switch S is in ON state, diodes  $D_1, D_2$  remain reverse biased and the following equations apply.

$$V_i = V_{L1} \tag{26}$$

$$V_{C2} = V_{C1} + V_{L1} \tag{27}$$

$$V_{CO} = V_C \tag{28}$$

Mode 2 Now S is in the OFF state and the following equation applies.

$$V_0 = V_{C1} + V_{C2} \tag{29}$$

Under steady state, below given equations can be derived.

$$\frac{V_{C2}}{V_i} = \frac{1}{1 - D} \tag{30}$$

$$\frac{V_0}{V_i} = \frac{1 + D}{1 - D} \tag{31}$$

Eq. (31) describes the gain equation of the converter.

Design considerations.

By Eq. (31), duty cycle  $D = 0.2$

By Eq. (16)  $L_1 = L_2 = 284\mu H$ ,

$$C_1 = \frac{I_0 D}{f_s \Delta V_{C1}} = 250\mu F$$

$$V_{C1} = \frac{V_i D}{1 - D} = 4V$$

Ripple voltage across capacitor  $C_1 = 5\%$  of  $= 0.2V$

Similarly,  $C_2 = \frac{I_0 D}{f_s \Delta V_{C2}} = 50\mu F$ ,  $V_{C2} = 20V$

$$C_0 = \frac{I_0 D}{\Delta V_0 f_s} = 41.6\mu F ; \Delta V_0 = 5\% \text{ of } V_0 = 1.2V$$

### 5. Discussion on the results

The three converters proposed for the comparative analysis in the test solar PV systems are operated by the proposed variable step size P&O MPPT controller. The complete system is modelled in MATLAB/Simulink. The system is sourced by an MSX 60 solar PV which is modelled based on electrical characteristics available in manufactures data sheets. Performance of the system with different converter topologies is analysed for various input circumstances.

#### 5.1 Standard Test Condition (STC)

Figure 8. shows the duty cycle of the three converter topologies when operated with the proposed controller by maintaining the irradiation to the PV module constant as  $1000W/m^2$  while the temperature kept constant as  $25^\circ C$ . It clearly shows the performance of the controller to track the duty cycle and that the steady state is attained at a faster rate when the system is operated with modified SEPIC. It is also inferred that when the system is operated with the proposed controller using modified SEPIC, the exact duty cycle of 0.2 is tracked.

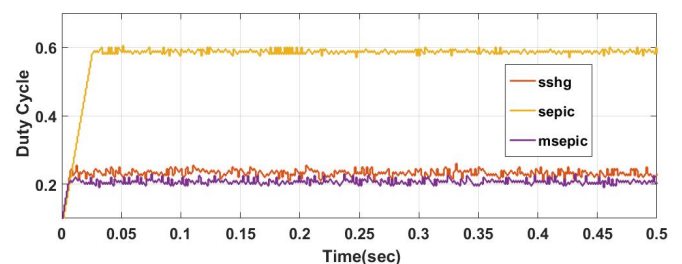


Figure 8. Duty cycle plot under STC

Figure 9 shows the output power of the system with the different converters under STC. Maximum output is transferred to the load with minimum oscillations when the system is operated with modified SEPIC converter. Percentage of ripple in the output power is inferred as maximum for the system with SEPIC converter.

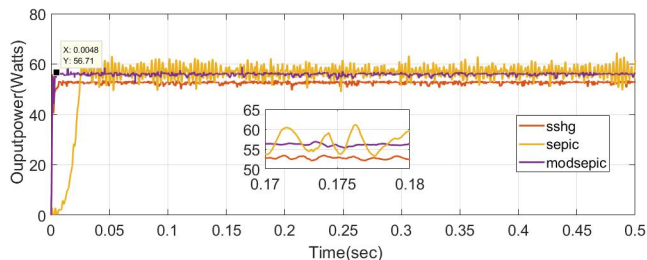


Figure 9. Output power plot under STC

Figure 10 and Fig. 11 shows the voltage plots at the input and output side of the converter under STC. Since the irradiation and temperature under this condition is maintained constant as 1000W/m<sup>2</sup> and 25°C respectively, output voltage plot does not exhibit much oscillations. Maximum average output voltage is made available across the load with minimum ripple when the PV system is operated with modified SEPIC converter. Percentage of ripple in the output voltage is found to be maximum when the system is operated with a SEPIC converter.

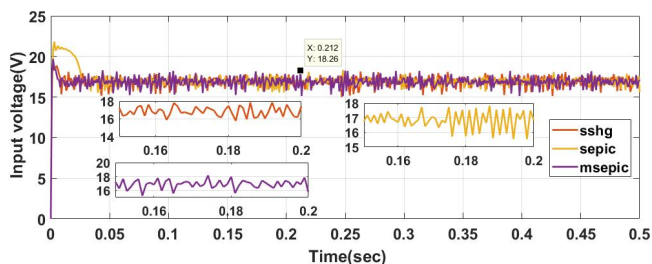


Figure 10. Input voltage under STC

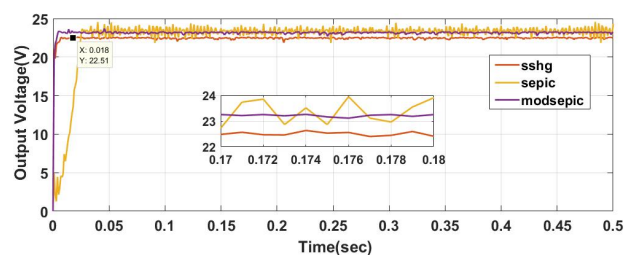


Figure 11. Output voltage of converter under STC

Plot of the current drawn by the converter under STC is shown in Fig. 12. Percentage of ripple in the input current is found to be minimum for modified SEPIC and maximum for SEPIC converter.

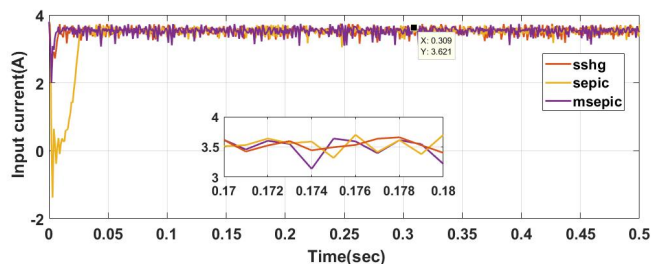


Figure 12 Input current plot under STC

The system performance under STC is found better with modified SEPIC converter with a minimum amount of ripple in the output power, output voltage, input current and it also exhibits maximum system efficiency.

### 5.2 Variable Irradiation Input Condition

Keeping the temperature value constant as 25°C, variations are applied to the irradiation at the input of the solar PV as 725W/m<sup>2</sup>, 1000W/m<sup>2</sup>, 860W/m<sup>2</sup> and 1120W/m<sup>2</sup> and each situation for a duration of 0.05 seconds and the system performance is monitored for 0.2 seconds. The applied changes in irradiation level is shown in Fig. 13.

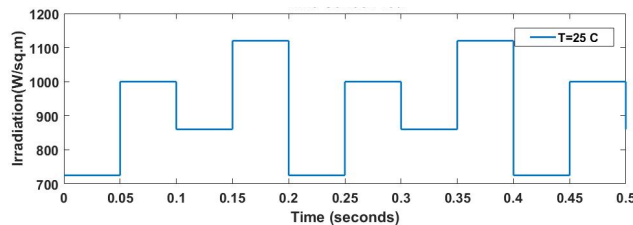


Figure 13. Plot of varying irradiation

Performance of the system for the stated input circumstances are inferred from the following duty cycle, power, voltage and current graphs obtained by making the system active for 0.2 seconds. Figure 14 shows the duty cycle of various converters used in the system. For an irradiation of 725W/m<sup>2</sup>, the proposed controller with SEPIC converter shows a comparatively slow response in attaining steady state compared to the rest two converters. Overall performance of the controller is better in the system with modified SEPIC in almost all conditions of variable irradiation.

Output power of the system with various converters is shown in Fig. 15. Though the temperature maintained constant output power shows variations as the irradiation to the module changes in every 0.05 seconds. For the entire duration, performance of the proposed controller in the system is superior with modified SEPIC converter, which could deliver more average power to load with least ripple content in it. A similar observation can be inferred from the plot of output voltage shown in Fig. 16, where the performance of the proposed controller in the system with modified SEPIC converter is superior in terms of the average value and ripple.

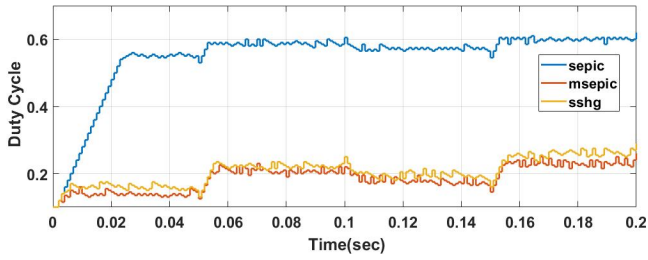


Figure 14. Duty cycle of various converters for varying irradiation

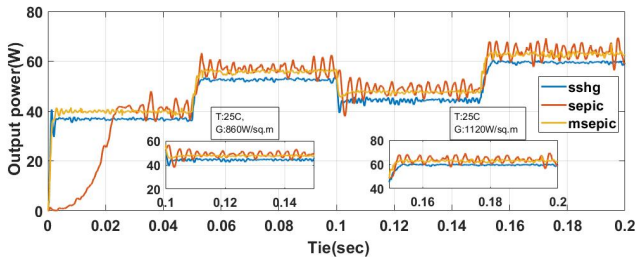


Figure 15. Output power delivered to the load

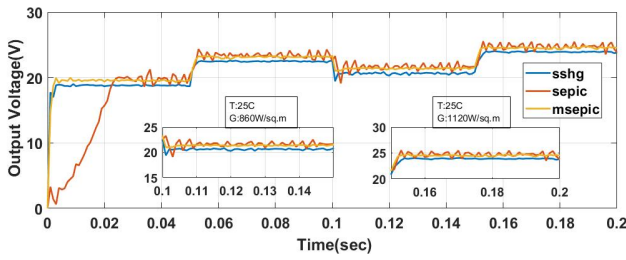


Figure 16. Plot of output voltage across load

Figure 17 shows the plot of input current drawn by the system with various converters. Under almost all conditions of varying irradiation, system performance with the controller is superior with modified SEPIC as the converter.

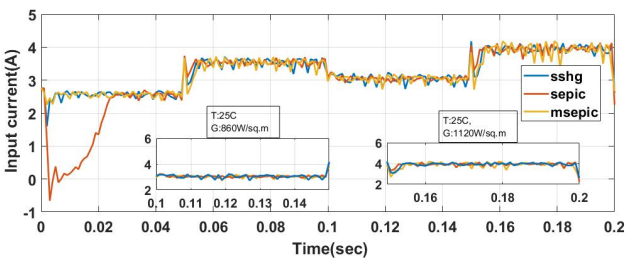


Figure 17. Input current plot for varying irradiation

### 5.3 Variable temperature Condition

Keeping the irradiation constant as 1000W/m<sup>2</sup>, the temperature input to the solar PV is varied as shown in Fig. 18 and the system is made to be active for 0.2 seconds. Figure 19 shows the duty cycle of the selected converters tracked by the proposed controller in the system. Performance of the controller in the system with SEPIC converter is noted to be inferior in reaching steady state, whereas that with modified SEPIC performs the best. Figure 20 displays the output power plot for the changing temperature condition. With regard to the average power output and its ripple content, the system with modified SEPIC converter exhibits superior

performance. The output voltage plots of various converters used in the PV system shown in Fig. 21 clarifies the superior performance of modified SEPIC converter in terms of its magnitude and ripple content. Current drawn by the chosen converters from the PV module is displayed in Fig. 22. In all the mentioned cases, a system with modified SEPIC converter exhibits a superior performance using the proposed controller. The following are the graphs derived which are used for analysis.

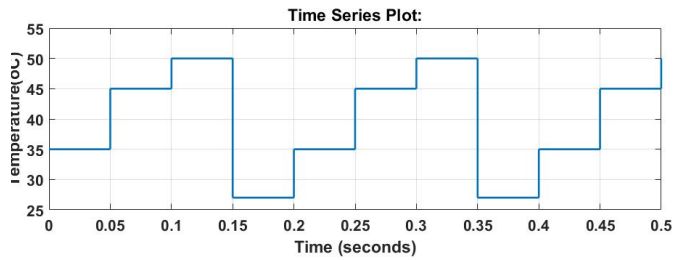


Figure 18. Plot of temperature variations at the input of the system

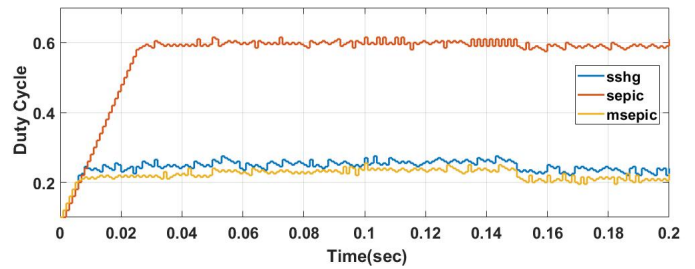


Figure 19. Duty cycle plot of the converters for the stated condition

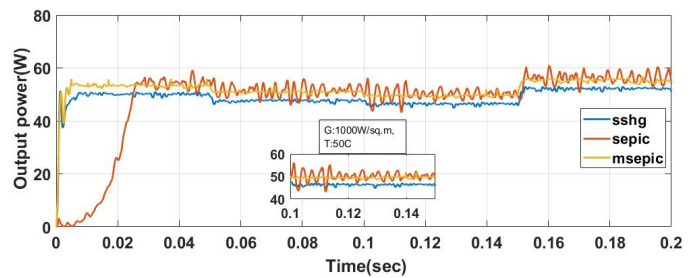


Figure 20. Output power plot

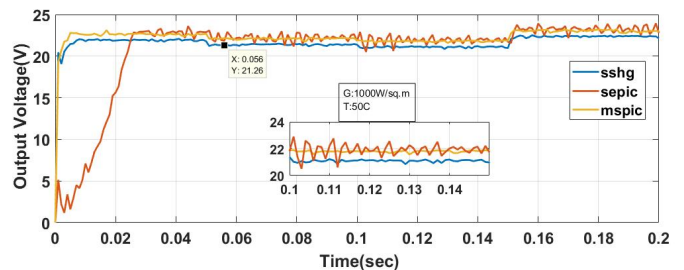


Figure 21. Output voltage plot

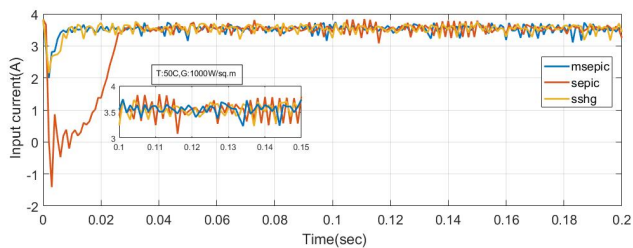


Figure 22. Input current plot

**6. Ripple analysis**

Based on the outcome from the numerical experiments for the above stated three different input circumstances of the solar PV, a comparison is made on the amount of ripples in output power, output voltage and input current. Also the system with three different converter topologies are compared on the basis of efficiency, which are tabulated below in table 1, 2 and 3.

Table 1. Standard test condition

| Converter               | SSHG  | SEPIC | Mod. SEPIC |
|-------------------------|-------|-------|------------|
| Input current ripple %  | 2.55  | 7.54  | 2.34       |
| Output voltage ripple % | 0.62  | 0.86  | 0.82       |
| Input power ripple %    | 2.47  | 2.73  | 1.19       |
| Output power ripple %   | 0.907 | 1.67  | 0.88       |
| Average efficiency %    | 90.21 | 96.08 | 96.71      |

Table 2. Variable irradiation

|                                 | SSHG  |       | SEPIC |       | Mod. SEPIC |       |
|---------------------------------|-------|-------|-------|-------|------------|-------|
|                                 | 1000  | 860   | 1000  | 860   | 1000       | 860   |
| Irradiation (W/m <sup>2</sup> ) | 1000  | 860   | 1000  | 860   | 1000       | 860   |
| Input current (A)               | 3.41  | 3.17  | 3.57  | 3.33  | 3.50       | 2.95  |
| Input current ripple (%)        | 2.55  | 2.96  | 7.54  | 5.31  | 2.34       | 1.93  |
| Output voltage (V)              | 22.58 | 20.16 | 23.33 | 19.72 | 23.12      | 21.42 |
| Output voltage ripple (%)       | 0.62  | 0.89  | 0.86  | 1.87  | 0.82       | 0.37  |
| Output power (W)                | 52.9  | 42.30 | 56.69 | 40.54 | 57.57      | 49.00 |
| Output power Ripple (%)         | 0.91  | 1.63  | 1.68  | 3.70  | 0.88       | 0.22  |
| Efficiency (%)                  | 90.22 | 89.57 | 96.08 | 93.67 | 96.71      | 95.80 |

Table 3. Variable temperature

|                            | SSHG  |       | SEPIC |       | Mod. SEPIC |       |
|----------------------------|-------|-------|-------|-------|------------|-------|
|                            | 35    | 50    | 35    | 50    | 35         | 50    |
| Temperature (°C)           | 35    | 50    | 35    | 50    | 35         | 50    |
| Average Input current (A)  | 3.53  | 3.56  | 3.49  | 3.44  | 3.59       | 3.69  |
| Input current ripple (%)   | 2.15  | 1.52  | 8.95  | 2.61  | 1.87       | 1.89  |
| Average Output voltage (V) | 22.05 | 21.15 | 22.72 | 21.03 | 22.73      | 21.58 |
| Output voltage ripple (%)  | 0.27  | 0.14  | 1.27  | 7.98  | 0.62       | 1.11  |
| Average Output power (W)   | 50.7  | 46.50 | 53.77 | 45.44 | 54.58      | 50.29 |
| Output power ripple (%)    | 0.24  | 0.69  | 2.58  | 13.16 | 1.55       | 1.11  |
| Efficiency (%)             | 88.72 | 87.82 | 94.82 | 96.14 | 95.64      | 96.48 |

**7. Conclusion**

The proposed variable step size P&O MPPT controller considered for the efficiency comparison of the three converter topologies in the developed PV system are done based on the parameters like ripple content in input current, output voltage and average power efficiency. Validating the results of Table 1., Table 2. and Table 3. clearly indicates that the performance of the modelled standalone PV system with modified SEPIC converter is superior, for almost all climatic conditions. Also the system with modified SEPIC topology with the proposed controller under STC promises an average efficiency of 96.71% which is more than the full load efficiency of the converter as stated already [12]. Moreover, the proposed controller in the system with modified SEPIC converter shows better and fast response in tracking duty cycle under varying air temperature and solar irradianations.

**References**

- [1] B. Pakkiraiah and G. D. Sukumar, " Research Survey on Various MPPT Performance Issues to improve the Solar PV System Efficiency", Journal of Solar Energy, vol. 2016, DOI: 10.1155/2016/8012432.
- [2] M.A. Husain, A. Tariq, S. Hameed, M.S.B. Arif and A. Jain, "Comparative assessment of maximum power point tracking procedures for photovoltaic systems", Green Energy & Environment, vol. 2, no.1, pp. 5-17, January 2016.
- [3] A. Al-Diab and C. Sourkounis, "Variable step size P&O MPPT algorithm for PV systems", 12th International Conference on Optimization of Electrical and Electronic Equipment, Basov, DOI: 10.1109/OPTIM.2010.551044, pp. 1097-1102, 2010.
- [4] T. Tsuji, A. Hidaka and S. Matsumoto, "A stand-alone power supply system using single photovoltaic cell with maximum power point tracking", International

- Conference on Renewable Energy Research and Applications, Nagasaki, DOI: 10.1109/ICRERA.2012.6477292, pp. 1-5, 2012.
- [5] Q. Deng, R. Alvarado, E. Toledo and L. Caraguay, "Greenhouse gas emissions, non-renewable energy consumption and output in South America: the role of the productive structure", *Environmental Science and Pollution Research*, vol. 27, pp. 14477-14491, 2020.
- [6] S. A. Gorji, (Member, IEEE), H. G. Sahebi, M. Ektesabi, (Member, IEEE) and A. B. Rad (Senior Member, IEEE)", *Topologies and Control Schemes of Bidirectional DC-DC Power Converters-An Overview*", *IEEE Access*, vol. 7, pp. 117997-118019, August 2019.
- [7] M. A. Danandeh and S. M. G. Mousavi, "Comparative and comprehensive review of maximum power point tracking methods for PV cells", *Renew. Sustain. Energy Rev.*, vol. 82, pp. 2743-2767, Feb. 2018.
- [8] Y. Wang, M. Zhang and X. Cheng, "An Improved MPPT Algorithm for PV Generation Applications Based on P-U Curve Reconstitution", *Journal of Control Science and Engineering*, vol. 2016, DOI: 10.1155/2016/3242069, 2016.
- [9] S. Paul, K. P. Jacob and J. Jacob, "Solar Photovoltaic System with High Gain DC to DC Converter and Maximum Power Point Tracking Controller", *Journal of Green Engineering*, vol. 10, no. 5, May 2020.
- [10] S. Saravanan and N. R. Babu, "Design and Development of Single Switch High Step-Up DC-DC Converter", *IEEE Journal of Emerging and Selected Topics in Power Electronics*, vol. 6, No. 2, June 2018.
- [11] T. Porselvi and M. Arounassalame, "A novel Single Switch High Gain dc-dc Converter", *8th IEEE India International Conference on Power Electronics (IICPE)*, India, DOI: 10.1109/IICPE.2018.8709508, pp. 1-6, 2018.
- [12] H. Suryatmojo, I. Dilianto, Suwito, R. Mardiyanto, E. Setijadi and D. C. Riawan, "Design and analysis of high gain modified SEPIC converter for photovoltaic applications", *IEEE International Conference on Innovative Research and Development*, Bangkok, pp. 1-6, DOI: 10.1109/ICIRD.2018.8376319, 2018.
- [13] S. S. Mohammed, "Modelling and Simulation of Photovoltaic module using MATLAB/Simulink", *International Journal of Chemical and Environmental Engineering*, vol. 2 no. 5, January 2011.
- [14] S. Shongwe and M. Hanif, "Comparative Analysis of Different Single-Diode PV Modelling Methods", *IEEE Journal of Photovoltaics*, vol. 5, no. 3, pp. 938-946, May 2015.
- [15] S. Salim and P. K. Abraham, "High Gain High Efficiency Single Switch DC-DC Converter for Green Power Source Conversion", *Journal of Power Electronics & Power Systems*, vol. 8, No 3, pp. 46-56, 2018.
- [16] M. T. Ahmed, M. R. Rashel, F. Faisal and M. Tlemçani, "Non-iterative MPPT Method-A Comparative Study", *International Journal of Renewable Energy Research*, vol. 10, No. 2, June 2020.
- [17] V. Rodolfo, (Member, IEEE), S. Romero, R. C. Ambrosio, (Member, IEEE), G. Mino, (Member, IEEE), E. Bonizzoni, (Senior Member, IEEE) and F. Maloberti, (Fellow, IEEE), "A Behavioural Model for Solar Cells with Transient Irradiation and Temperature Assessment", *IEEE Access*, vol. 7, pp. 90882-90890, July 2019.
- [18] Vinod, R. Kumar and S.K.Singh, "Solar photovoltaic modelling and simulation-As a renewable energy solution," *Energy Reports* 4, pp. 701-712, 2018.
- [19] M. R. Rashel, A. Albino, M. Tlemçani, T. C. F. Gonçalves and J. Rifath, "MATLAB Simulink modeling of photovoltaic cells for understanding shadow effect", *IEEE International Conference on Renewable Energy Research and Applications*, Birmingham, 2016, pp. 747-750, 2016.
- [20] X.H. Nguyen and M.P. Nguyen, "Mathematical modelling of photovoltaic cell/module/arrays with tags in Matlab/Simulink", *Environ Systems and Research*, vol. 4, no. 24, DOI: 10.1186/s40068-015-0047-9, 2015.
- [21] M.R. Zekry, M.M. Sayed, K.M. Hosam and Yousef, "Comparative study of maximum power point tracking methods for photovoltaic system ", *Journal of Electrical Engineering*, January 2015.
- [22] M. Alqarni and M. K. Darwish, "Maximum power point tracking for photovoltaic system: Modified Perturb and Observe algorithm", *47th International Universities Power Engineering Conference* pp. 1-4, 2012.
- [23] F. L. Tofoli, D. C. Pereira, and W. J. Paula, "Comparative Study of Maximum Power Point Tracking Techniques for Photovoltaic Systems", *International Journal of Photo energy*, vol. 2015, pp. 1-10, January 2015.
- [24] M. A. G. Brito, L. Galotto, L. P. Sampaio, G. A. Melo and C. A. Canesin, "Evaluation of the Main MPPT Techniques for Photovoltaic Applications", *IEEE Transactions on Industrial Electronics*, vol. 60, issue 3, pp. 1156 - 1167, March 2013.
- [25] H. A. Sher, A. F. Murtaza, A. Noman, K. E. Addoweesh, and K. Al-Haddad, "A New Sensorless Hybrid MPPT Algorithm Based on Fractional Short-Circuit Current Measurement and P&O MPPT", *IEEE Transactions on Sustainable Energy*, vol. 6, pp. 1426 - 1434, 2015.
- [26] A. Ali, A. N. Hasan and T. Marwala, "Perturb and observe based on fuzzy logic controller maximum power point tracking (MPPT)", *International Conference on Renewable Energy Research and Application*, 19-22 Oct. 2014.
- [27] A. A. Abdalla and M. Khalid, "Smoothing Methodologies for Photovoltaic Power Fluctuations", *8th International Conference on Renewable Energy Research and Applications*, 3-6 November, 2019.
- [28] M. A. Abdourraziq, M. Ouassaid, M. Maaroufi and S. Abdourraziq, "Modified P&O MPPT technique for photovoltaic systems", *International Conference on*

- Renewable Energy Research and Applications, pp. 728-733, 20-23 October 2013.
- [29] M. Abdel-Salam, M.T. El-Mohandes and M. Goda, "An improved perturb-and-observe based MPPT method for PV systems under varying irradiation levels", *Solar Energy*, vol. 171, pp. 547-561, Sep. 2018.
- [30] L. Xingshuo, (Student Member, IEEE), Q. Wang, H. Wen, (Senior Member, IEEE) and W. Xiao, (Member, IEEE), "Comprehensive Studies on Operational Principles for Maximum Power Point Tracking in Photovoltaic Systems", *IEEE Special Section On Emerging Technologies for Energy Internet*, vol. 7, pp. 121407-121420, 2019.
- [31] H. Bahri, and A. Harrag, "Variable Step Size P&O MPPT Controller to Improve Static and Dynamic PV System Performances", *Journal of Advanced Engineering and Computation*, vol. 2, pp. 86-93, June 2018.
- [32] P. Saadat, and K. Abbaszadeh, "A Single-Switch High Step-Up DC-DC Converter Based on Quadratic Boost", *IEEE Transactions on Industrial Electronics*, vol. 63, no. 12, pp. 7733-7742, Dec. 2016.
- [33] P. K. Maroti, S. Padmanaban, J. B. Holm-Nielsen, M. S. Bhaskar, M. Meraj and A. Iqbal, "A New Structure of High Voltage Gain SEPIC Converter for Renewable Energy Applications", *IEEE Access*, vol. 7, pp. 89857-89868, 2019.
- [34] Geeta and R. Hemavathi, "Design and Simulation of Closed Loop SEPIC DC-DC Converter for a Stand-alone Photovoltaic System", *International Journal of Advanced Research in Electrical, Electronics and Instrumentation Engineering*, vol. 7, no. 10, October 2018.
- [35] S. Paul, N. SunilKumar and J. Jacob, "Solar PV System with Modified High Gain SEPIC Converter and Multiple Step Size P&O MPPT Technique", *International Journal of Advanced Science and Technology*, vol. 29, no. 8, pp. 4065-4075, 2020.